

Static and Free Vibration Analysis of Thin Plates of the Curved Edges by the Boundary Element Method Considering an Alternative Formulation of Boundary Conditions

Michał GUMINIAK

Poznan University of Technology
Piotrowo 5, 60-965 Poznań, Poland
e-mail: michal.guminiak@put.poznan.pl

A static and dynamic analysis of Kirchhoff plates is presented in this paper. The proposed approach avoids Kirchhoff forces at the plate corners and equivalent shear forces at a plate boundary. Two unknown variables are considered at the boundary element node. The governing integral equations are derived using Betti's theorem. The rectilinear and curved boundary element of the constant type are used. The non-singular formulation of the boundary (static analysis) and boundary-domain (free vibration analysis) integral equations with one and two collocation points associated with a single constant boundary element located at a plate edge are presented. Additionally, the classic three-node isoparametric curved boundary elements are introduced in static analysis according to the non-singular approach. Static fundamental solution and Bèzine technique are applied to the free vibration analysis. To establish the plate inertial forces, a plate domain is divided into triangular or annular sub-domains associated with one suitable collocation point.

Key words: Boundary Element Method, Kirchhoff plates, fundamental solution.

1. INTRODUCTION

The Boundary Element Method (BEM) was created as an independent numerical tool to solve problems, e.g., in the field of potential theory, theory of elasticity, and engineering theory of structures. In its purest approach the BEM does not require the entire domain discretization but only the boundary of a considered structure. The main advantage of BEM is its simplicity of computational algorithms in relation to engineering problems. The general application of BEM in a variety of fields of engineering analysis, together with the appropriate solutions and a discussion of the basic types of boundary elements was described

by BURCZYŃSKI [1], WROBEL and ALIABADI [2], and KATSIKADELIS [3]. Many authors applied the BEM widely to static, dynamic, and stability analysis of plates, e.g., ALTIERO and SIKARSKIE [4], BÈZINE and GAMBY [5], STERN [6], and HARTMANN and ZOTEMANTEL [7]. A comparison of the effectiveness of the Boundary Element Method with the Finite Element Method and application of BEM in the analysis of thick plates was carried out by DEBBIH [8, 9]. The dynamic analysis of plates according to BEM algorithms was presented by BESKOS [10] and WEN, ALIABADI and YOUNG [11]. SHI [12] applied BEM formulation for vibration and initial stability problems of orthotropic thin plates. MYŚLECKI and OLEŃKIEWICZ [13, 14] used the non-singular approach of boundary integral equations to free vibration analysis of thin plates wherein the derivation of the second boundary integral equation was executed for additional collocation points located outside of a plate domain. A number of contributions devoted to the analysis of plates was presented by: KATSIKADELIS [15, 16], KATSIKADELIS, SAPOUNTZAKIS and ZORBA [17], KATSIKADELIS and KANDILAS [18], KATSIKADELIS and SAPOUNTZAKIS [19]. A modified, simplified formulation of the boundary integral equation for a thin plate was proposed by GUMINIAK [20]. This approach was applied to a dynamic analysis of thin plates [21–24]. Sygulski presented a number of publications devoted to the analysis of fluid-structure interaction, which was described widely in [25]. The author connected FEM and BEM to solve dynamic influence of surrounding air on a pneumatic shell with application of original computational algorithms.

The conception of the Analog Equation Method (AEM) was created and introduced by KATSIKADELIS [26] to fully overcome the major drawback of the BEM in pure form, which is its limitation to linear problems with known fundamental solutions. This version of BEM is based on a formulation of the boundary-domain integral equation method and can efficiently treat not only linear problems whose fundamental solution cannot be established or is difficult to treat numerically but also nonlinear differential equations and systems of them as well. BABOUSKOS and KATSIKADELIS [27, 28] applied AEM and BEM methodology to solve the problem of a flutter instability of the dumped plate subjected by conservative and non-conservative loading. Application of the rectilinear and curvilinear boundary elements in static analysis of plates was presented in papers [29–31].

In the present paper, the static and dynamic analysis of plate by the BEM will be presented. The analysis will focus on the modified formulation of the governing boundary-domain integral equation in thin plate bending. The rectilinear and curvilinear boundary elements will be applied in the analysis. The BÈZINE [5] technique will be applied to derive directly the boundary-domain integral equation.

2. INTEGRAL FORMULATION OF A PLATE BENDING AND STATIC PROBLEM

The differential equation governing the static bending of isotropic plates with constant thickness has the known form [32]

$$(2.1) \quad D \cdot \nabla^4 w(x, y) = p(x, y),$$

where $D = \frac{Eh^3}{12(1-\nu^2)}$ is the plate stiffness, h is plate thickness, E and ν are the Young modulus and the Poisson ratio.

In the majority of contributions devoted to the application of BEM to the thin (Kirchhoff) plate theory, the derivation of the boundary integral equation involves the known boundary variables of the classic plate theory, i.e. the shear force and the concentrated corner forces. Thus, on the plate boundary two physical quantities are considered: the equivalent shear force V_n , reaction at the plate k -th corner R_k , the bending moment M_n , the corner concentrated forces, and two geometric variables: the displacement w_b and the angle of rotation in the normal direction φ_n . The solution of differential Eq. (2.1) can be expressed in the form of an integral representation as two boundary integral equations. These equations can also be derived directly using Betti's theorem. Two plates are considered: an infinite plate, subjected to the unit concentrated force and a real one, subjected to the real loading $p(x, y)$. The first equation has the form:

$$(2.2) \quad c(\mathbf{x}) \cdot w(\mathbf{x}) + \int_{\Gamma} [V_n^*(\mathbf{y}, \mathbf{x}) \cdot w_b(\mathbf{y}) - M_n^*(\mathbf{y}, \mathbf{x}) \cdot \varphi_n(\mathbf{y})] \cdot d\Gamma(\mathbf{y}) \\ - \sum_{k=1}^K R_k^*(k, \mathbf{x}) \cdot w(k) = \int_{\Gamma} [V_n(\mathbf{y}) \cdot w^*(\mathbf{y}, \mathbf{x}) - M_n(\mathbf{y}, \mathbf{x}) \cdot \varphi_n^*(\mathbf{y}, \mathbf{x})] \cdot d\Gamma(\mathbf{y}) \\ - \sum_{k=1}^K R_k \cdot w^*(k, \mathbf{x}) + \int_{\Omega} p(\mathbf{y}) \cdot w^*(\mathbf{y}, \mathbf{x}) \cdot d\Omega(\mathbf{y}),$$

where the fundamental solution of this biharmonic equation

$$(2.3) \quad \nabla^4 w^*(\mathbf{y}, \mathbf{x}) = \frac{1}{D} \cdot \delta(\mathbf{y}, \mathbf{x}),$$

which is the free space Green function given as

$$(2.4) \quad w^*(\mathbf{y}, \mathbf{x}) = \frac{1}{8\pi D} \cdot r^2 \cdot \ln(r)$$

for a thin isotropic plate, $r = |\mathbf{y} - \mathbf{x}|$, δ is the Dirac delta, \mathbf{x} is the source point, and \mathbf{y} is a field point. The coefficient $c(\mathbf{x})$ is taken as:

- $c(\mathbf{x}) = 1$, when \mathbf{x} is located inside the plate domain,
- $c(\mathbf{x}) = 0.5$, when \mathbf{x} is located on the smooth boundary,
- $c(\mathbf{x}) = 0$, when \mathbf{x} is located outside the plate domain.

The second boundary integral equation can be obtained by replacing the unit concentrated force $P^* = 1$ by the unit concentrated moment $M_n^* = 1$. Such the replacement is equivalent to the differentiation of the first boundary integral Eq. (2.2) with respect to the co-ordinate n at a point \mathbf{x} belonging to the plate domain and letting this point approach the boundary and taking n coincide with the normal to it. The resulting equation has the form:

$$(2.5) \quad c(\mathbf{x}) \cdot \varphi_n(\mathbf{x}) + \int_{\Gamma} \left[\overline{V}_n^*(\mathbf{y}, \mathbf{x}) \cdot w_b(\mathbf{y}) - \overline{M}_n^*(\mathbf{y}, \mathbf{x}) \cdot \varphi_n(\mathbf{y}) \right] \cdot d\Gamma(\mathbf{y}) \\ - \sum_{k=1}^K \overline{R}^*(k, \mathbf{x}) \cdot w(k) = \int_{\Gamma} [V_n(\mathbf{y}) \cdot \overline{w}^*(\mathbf{y}, \mathbf{x}) - M_n(\mathbf{y}) \cdot \overline{\varphi}_n^*(\mathbf{y}, \mathbf{x})] \cdot d\Gamma(\mathbf{y}) \\ - \sum_{k=1}^K R_k \cdot \overline{w}^*(k, \mathbf{x}) + \int_{\Omega} p(\mathbf{y}) \cdot \overline{w}^*(\mathbf{y}, \mathbf{x}) \cdot d\Omega(\mathbf{y}),$$

where

$$\left\{ \overline{V}_n^*(\mathbf{y}, \mathbf{x}), \overline{M}_n^*(\mathbf{y}, \mathbf{x}), \overline{R}^*(\mathbf{y}, \mathbf{x}), \overline{w}^*(\mathbf{y}, \mathbf{x}), \overline{\varphi}_n^*(\mathbf{y}, \mathbf{x}) \right\} \\ = \frac{\partial}{\partial n(\mathbf{x})} \{ V_n^*(\mathbf{y}, \mathbf{x}), M_n^*(\mathbf{y}, \mathbf{x}), R^*(k, \mathbf{x}), w^*(k, \mathbf{x}), w^*(\mathbf{y}, \mathbf{x}), \varphi_n^*(\mathbf{y}, \mathbf{x}) \}.$$

The second boundary integral equation can be also derived by introducing an additional collocation point which is located in the same normal line outside the plate edge. According to this approach, the second equation has the same mathematical form as the first one (2.2). This double collocation point approach was presented in publication [13, 14]. The issues related to the assembly of the algebraic equations in terms of the classical Boundary Element Method are discussed in many papers, e.g. [3].

The plate bending problem can be also formulated in the modified, simplified way, using an integral representation of the plate biharmonic equation. Because the concentrated force at the corner is used only to satisfy the differential biharmonic equation of the thin plate, one can assume that it could be distributed along a plate edge segment close to the corner [30]. Hence, terms in the boundary integral Eqs. (2.2) and (2.5) which correspond to the corner force R can be substituted in the following way:

$$(2.6) \quad - \sum_{k=1}^K R_k \cdot w^*(k, \mathbf{x}) = \int_{\Gamma_k} R_n(\mathbf{y}) \cdot w^*(\mathbf{y}, \mathbf{x}) \cdot d\Gamma_k(\mathbf{y}),$$

$$(2.7) \quad - \sum_{k=1}^K R_k \cdot \bar{w}^*(k, \mathbf{x}) = \int_{\Gamma_k} R_n(\mathbf{y}) \cdot \bar{w}^*(\mathbf{y}, \mathbf{x}) \cdot d\Gamma_k(\mathbf{y}),$$

where the subscript k denotes an unknown segment of the plate edge near the corner. In the Eqs. (2.2) and (2.5) the fundamental twisting moment $M_{ns}^*(\mathbf{y})$ must be considered, too. Hence, the boundary integral equations will take the form:

$$(2.8) \quad c(\mathbf{x}) \cdot w(\mathbf{x}) + \int_{\Gamma} [T_n^*(\mathbf{y}, \mathbf{x}) \cdot w(\mathbf{y}) - M_n^*(\mathbf{y}, \mathbf{x}) \cdot \varphi_n(\mathbf{y}) - M_{ns}^*(\mathbf{y}, \mathbf{x}) \cdot \varphi_s(\mathbf{y})] \\ \cdot d\Gamma(\mathbf{y}) = \int_{\Gamma} [T_n(\mathbf{y}) \cdot w^*(\mathbf{y}, \mathbf{x}) - M_n(\mathbf{y}) \cdot \varphi_n^*(\mathbf{y}, \mathbf{x})] \cdot d\Gamma(\mathbf{y}) \\ + \int_{\Gamma_k} R_n(\mathbf{y}) \cdot w^*(\mathbf{y}, \mathbf{x}) \cdot d\Gamma_k(\mathbf{y}) + \int_{\Omega} p(\mathbf{y}) \cdot w^*(\mathbf{y}, \mathbf{x}) \cdot d\Omega(\mathbf{y}),$$

$$(2.9) \quad c(\mathbf{x}) \cdot \varphi_n(\mathbf{x}) + \int_{\Gamma} [\bar{T}_n^*(\mathbf{y}, \mathbf{x}) \cdot w(\mathbf{y}) - \bar{M}_n^*(\mathbf{y}, \mathbf{x}) \cdot \varphi_n(\mathbf{y}) - \bar{M}_{ns}^*(\mathbf{y}, \mathbf{x}) \cdot \varphi_s(\mathbf{y})] \\ \cdot d\Gamma(\mathbf{y}) = \int_{\Gamma} [T_n(\mathbf{y}) \cdot \bar{w}^*(\mathbf{y}, \mathbf{x}) - M_n(\mathbf{y}) \cdot \bar{\varphi}_n^*(\mathbf{y}, \mathbf{x})] \cdot d\Gamma(\mathbf{y}) \\ + \int_{\Gamma_k} R_n(\mathbf{y}) \cdot \bar{w}^*(\mathbf{y}, \mathbf{x}) \cdot d\Gamma_k(\mathbf{y}) + \int_{\Omega} p(\mathbf{y}) \cdot \bar{w}^*(\mathbf{y}, \mathbf{x}) \cdot d\Omega(\mathbf{y}).$$

The length k of the plate edge segment is unknown. It allows us to include components

$$\int_{\Gamma} [T_n(\mathbf{y}) \cdot w^*(\mathbf{y}, \mathbf{x})] \cdot d\Gamma(\mathbf{y}) \quad \text{with} \quad \int_{\Gamma_k} R_n(\mathbf{y}) \cdot w^*(\mathbf{y}, \mathbf{x}) \cdot d\Gamma_k(\mathbf{y})$$

and

$$\int_{\Gamma} [T_n(\mathbf{y}) \cdot \bar{w}^*(\mathbf{y}, \mathbf{x})] \cdot d\Gamma(\mathbf{y}) \quad \text{with} \quad \int_{\Gamma_k} R_n(\mathbf{y}) \cdot \bar{w}^*(\mathbf{y}, \mathbf{x}) \cdot d\Gamma_k(\mathbf{y})$$

under the common integral:

$$(2.10) \quad c(\mathbf{x}) \cdot w(\mathbf{x}) + \int_{\Gamma} [T_n^*(\mathbf{y}, \mathbf{x}) \cdot w(\mathbf{y}) - M_n^*(\mathbf{y}, \mathbf{x}) \cdot \varphi_n(\mathbf{y}) - M_{ns}^*(\mathbf{y}, \mathbf{x}) \cdot \varphi_s(\mathbf{y})] \\ \cdot d\Gamma(\mathbf{y}) = \int_{\Gamma} [T_n(\mathbf{y}) \cdot w^*(\mathbf{y}, \mathbf{x}) + R_n(\mathbf{y}) \cdot w^*(\mathbf{y}, \mathbf{x}) - M_n(\mathbf{y}) \cdot \varphi_n^*(\mathbf{y}, \mathbf{x})] \cdot d\Gamma(\mathbf{y}) \\ + \int_{\Omega} p(\mathbf{y}) \cdot w^*(\mathbf{y}, \mathbf{x}) \cdot d\Omega(\mathbf{y}),$$

$$(2.11) \quad c(\mathbf{x}) \cdot \varphi_n(\mathbf{x}) + \int_{\Gamma} [\overline{T}_n^*(\mathbf{y}, \mathbf{x}) \cdot w(\mathbf{y}) - \overline{M}_n^*(\mathbf{y}, \mathbf{x}) \cdot \varphi_n(\mathbf{y}) - \overline{M}_{ns}^*(\mathbf{y}, \mathbf{x}) \cdot \varphi_s(\mathbf{y})] \\ \cdot d\Gamma(\mathbf{y}) = \int_{\Gamma} [T_n(\mathbf{y}) \cdot \overline{w}^*(\mathbf{y}, \mathbf{x}) + R_n(\mathbf{y}) \cdot \overline{w}^*(\mathbf{y}, \mathbf{x}) - M_n(\mathbf{y}) \cdot \overline{\varphi}_n^*(\mathbf{y}, \mathbf{x})] \cdot d\Gamma(\mathbf{y}) \\ + \int_{\Omega} p(\mathbf{y}) \cdot \overline{w}^*(\mathbf{y}, \mathbf{x}) \cdot d\Omega(\mathbf{y}).$$

After separating the common factors $w^*(\mathbf{y}, \mathbf{x})$ and $\overline{w}^*(\mathbf{y}, \mathbf{x})$ in Eqs. (2.10) and (2.11), respectively, these equations will take following forms:

$$(2.12) \quad c(\mathbf{x}) \cdot w(\mathbf{x}) + \int_{\Gamma} [T_n^*(\mathbf{y}, \mathbf{x}) \cdot w(\mathbf{y}) - M_n^*(\mathbf{y}, \mathbf{x}) \cdot \varphi_n(\mathbf{y}) - M_{ns}^*(\mathbf{y}, \mathbf{x}) \cdot \varphi_s(\mathbf{y})] \\ \cdot d\Gamma(\mathbf{y}) = \int_{\Gamma} [(T_n(\mathbf{y}) + R_n(\mathbf{y})) \cdot w^*(\mathbf{y}, \mathbf{x}) - M_n(\mathbf{y}) \cdot \varphi_n^*(\mathbf{y}, \mathbf{x})] \cdot d\Gamma(\mathbf{y}) \\ + \int_{\Omega} p(\mathbf{y}) \cdot w^*(\mathbf{y}, \mathbf{x}) \cdot d\Omega(\mathbf{y}),$$

$$(2.13) \quad c(\mathbf{x}) \cdot \varphi_n(\mathbf{x}) + \int_{\Gamma} [\overline{T}_n^*(\mathbf{y}, \mathbf{x}) \cdot w(\mathbf{y}) - \overline{M}_n^*(\mathbf{y}, \mathbf{x}) \cdot \varphi_n(\mathbf{y}) - \overline{M}_{ns}^*(\mathbf{y}, \mathbf{x}) \cdot \varphi_s(\mathbf{y})] \\ \cdot d\Gamma(\mathbf{y}) = \int_{\Gamma} [(T_n(\mathbf{y}) + R_n(\mathbf{y})) \cdot \overline{w}^*(\mathbf{y}, \mathbf{x}) - M_n(\mathbf{y}) \cdot \overline{\varphi}_n^*(\mathbf{y}, \mathbf{x})] \cdot d\Gamma(\mathbf{y}) \\ + \int_{\Omega} p(\mathbf{y}) \cdot \overline{w}^*(\mathbf{y}, \mathbf{x}) \cdot d\Omega(\mathbf{y}).$$

After introducing the new notation

$$(2.14) \quad \tilde{T}_n(\mathbf{y}) = T_n(\mathbf{y}) + R_n(\mathbf{y})$$

the boundary integral Eqs. (2.12) and (2.13) will have the following forms:

$$(2.15) \quad c(\mathbf{x}) \cdot w(\mathbf{x}) + \int_{\Gamma} [T_n^*(\mathbf{y}, \mathbf{x}) \cdot w(\mathbf{y}) - M_n^*(\mathbf{y}, \mathbf{x}) \cdot \varphi_n(\mathbf{y}) - M_{ns}^*(\mathbf{y}, \mathbf{x}) \cdot \varphi_s(\mathbf{y})] \\ \cdot d\Gamma(\mathbf{y}) = \int_{\Gamma} [\tilde{T}_n(\mathbf{y}) \cdot w^*(\mathbf{y}, \mathbf{x}) - M_n(\mathbf{y}) \cdot \varphi_n^*(\mathbf{y}, \mathbf{x})] \cdot d\Gamma(\mathbf{y}) \\ + \int_{\Omega} p(\mathbf{y}) \cdot w^*(\mathbf{y}, \mathbf{x}) \cdot d\Omega(\mathbf{y}),$$

$$(2.16) \quad c(\mathbf{x}) \cdot \varphi_n(\mathbf{x}) + \int_{\Gamma} [\bar{T}_n^*(\mathbf{y}, \mathbf{x}) \cdot w(\mathbf{y}) - \bar{M}_n^*(\mathbf{y}, \mathbf{x}) \cdot \varphi_n(\mathbf{y}) - \bar{M}_{ns}^*(\mathbf{y}, \mathbf{x}) \cdot \varphi_s(\mathbf{y})] \\ \cdot d\Gamma(\mathbf{y}) = \int_{\Gamma} [\tilde{T}_n(\mathbf{y}) \cdot \bar{w}^*(\mathbf{y}, \mathbf{x}) - M_n(\mathbf{y}) \cdot \bar{\varphi}_n^*(\mathbf{y}, \mathbf{x})] \cdot d\Gamma(\mathbf{y}) \\ + \int_{\Omega} p(\mathbf{y}) \cdot \bar{w}^*(\mathbf{y}, \mathbf{x}) \cdot d\Omega(\mathbf{y}).$$

The expression (2.14) denotes shear force for clamped and for simply-supported edges:

$$\tilde{T}_n(\mathbf{y}) = \begin{cases} V_n(\mathbf{y}) & \text{on the boundary far from the corner,} \\ R_n(\mathbf{y}) & \text{on a small fragment of the boundary close to the corner.} \end{cases}$$

Because in all the cases (Eqs. (2.2), (2.5) and (2.15), (2.16)) the forces on the real plate: $V_n(\mathbf{y})$ and $T_n(\mathbf{y})$ are multiplied by the same fundamental functions $w^*(\mathbf{y}, \mathbf{x})$ and $\bar{w}^*(\mathbf{y}, \mathbf{x})$, the force $\tilde{T}_n(\mathbf{y})$ can be treated as an equivalent shear force $V_n(\mathbf{y})$ on a fragment of the boundary which is located far from the corner. In the case of the free edge we must combine the angle of rotation in the tangent direction $\varphi_s(\mathbf{y})$ with the fundamental function $M_{ns}^*(\mathbf{y})$. The relation between $\varphi_s(\mathbf{y})$ and the deflection is known: $\varphi_s(\mathbf{y}) = \frac{dw(\mathbf{y})}{ds}$, the angle of rotation $\varphi_s(\mathbf{y})$ can be evaluated using the finite difference scheme and deflections with two or more adjacent nodal values. In this analysis, the employed finite difference scheme includes the deflections of two adjacent nodes. As a result, the boundary integral Eqs. (2.15) and (2.16) will take the forms:

$$(2.17) \quad c(\mathbf{x}) \cdot w(\mathbf{x}) + \int_{\Gamma} \left[T_n^*(\mathbf{y}, \mathbf{x}) \cdot w(\mathbf{y}) - M_{ns}^*(\mathbf{y}, \mathbf{x}) \cdot \frac{dw(\mathbf{y})}{ds} - M_n^*(\mathbf{y}, \mathbf{x}) \cdot \varphi_n(\mathbf{y}) \right] \cdot d\Gamma(\mathbf{y}) = \int_{\Gamma} \left[\tilde{T}_n(\mathbf{y}) \cdot w^*(\mathbf{y}, \mathbf{x}) - M_n(\mathbf{y}) \cdot \varphi_n^*(\mathbf{y}, \mathbf{x}) \right] \cdot d\Gamma(\mathbf{y}) + \int_{\Omega} p(\mathbf{y}) \cdot w^*(\mathbf{y}, \mathbf{x}) \cdot d\Omega(\mathbf{y}),$$

$$(2.18) \quad c(\mathbf{x}) \cdot \varphi_n(\mathbf{x}) + \int_{\Gamma} \left[\bar{T}_n^*(\mathbf{y}, \mathbf{x}) \cdot w(\mathbf{y}) - \bar{M}_{ns}^*(\mathbf{y}, \mathbf{x}) \cdot \frac{dw(\mathbf{y})}{ds} - \bar{M}_n^*(\mathbf{y}, \mathbf{x}) \cdot \varphi_n(\mathbf{y}) \right] \cdot d\Gamma(\mathbf{y}) = \int_{\Gamma} \left[\tilde{T}_n(\mathbf{y}) \cdot \bar{w}^*(\mathbf{y}, \mathbf{x}) - M_n(\mathbf{y}) \cdot \bar{\varphi}_n^*(\mathbf{y}, \mathbf{x}) \right] \cdot d\Gamma(\mathbf{y}) + \int_{\Omega} p(\mathbf{y}) \cdot \bar{w}^*(\mathbf{y}, \mathbf{x}) \cdot d\Omega(\mathbf{y}).$$

2.1. Types of boundary element

According to the simplest approach, the rectilinear boundary element of the constant type is introduced (Fig. 1a). It is also possible to define geometry of the element considering three nodal points and only one collocation point connected with a relevant physical boundary value (Fig. 1b). The collocation point may be located slightly outside of a plate edge. The geometry of the element can be defined by the polynomial functions (shape functions), described in standard

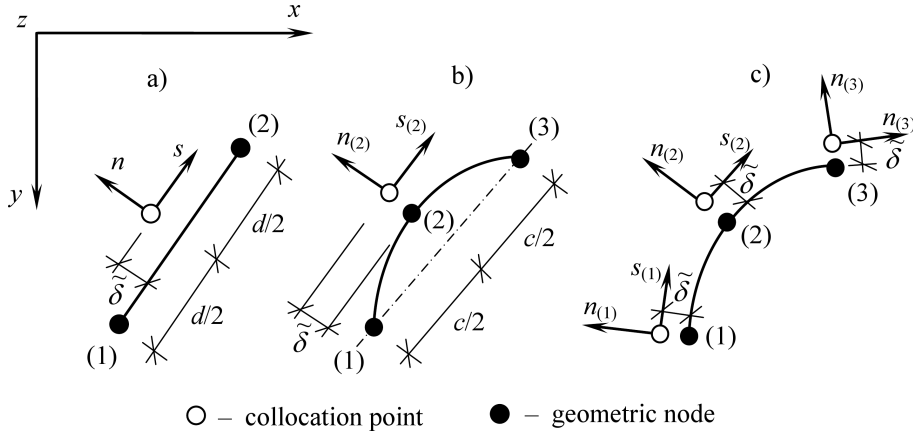


FIG. 1. Boundary elements in non-singular approach.

coordinate system for $\eta \in \langle -1, 0, 1 \rangle$ (Fig. 2). These functions have a known form:

$$(2.19) \quad \begin{aligned} N_1(\eta) &= \frac{1}{2}\eta \cdot (\eta - 1), \\ N_2(\eta) &= 1 - \eta^2, \\ N_3(\eta) &= -\frac{1}{2}\eta \cdot (\eta - 1). \end{aligned}$$

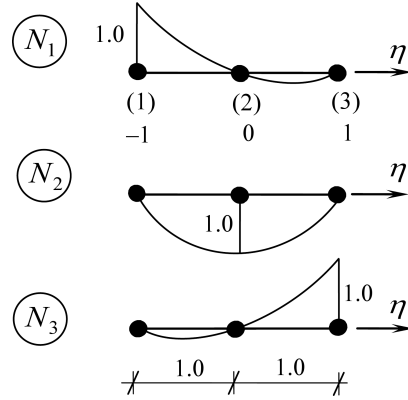


FIG. 2. Shape functions for three-node boundary element.

The isoparametric curved boundary element is shown in Fig. 1c. In this case, any boundary variable $B(\eta)$ is described by functions (2.19):

$$(2.20) \quad B(\eta) = B_1 \cdot N_1(\eta) + B_2 \cdot N_2(\eta) + B_3 \cdot N_3(\eta).$$

2.2. Assembly of a set of algebraic equations

A plate edge is discretized using boundary elements. In a matrix notation the set of algebraic equations has the form:

$$(2.21) \quad \mathbf{G} \cdot \bar{\mathbf{B}} = \mathbf{F},$$

where \mathbf{G} is a matrix of suitable boundary integrals, $\bar{\mathbf{B}}$ is the vector on unknown variables and \mathbf{F} is right-hand-side vector. If on the part of a plate boundary free edge takes place, then Eq. (2.21) may be prescribed to the form:

$$(2.22) \quad \begin{bmatrix} \mathbf{G}_{\text{BB}} & \mathbf{G}_{\text{BS}} \\ \Delta & -\mathbf{I} \end{bmatrix} \cdot \begin{Bmatrix} \mathbf{B} \\ \varphi_s \end{Bmatrix} = \begin{Bmatrix} \mathbf{F}_{\text{B}} \\ \mathbf{0} \end{Bmatrix},$$

where

\mathbf{B} is the boundary variables vector (column matrix) of the dimension $(2N \times 1)$, where N is the number of boundary nodes (or the number of the elements of the constant type);

φ_s is the vector (column matrix) of boundary angles of rotation in tangent direction depending on boundary deflections, this vector has the dimension $(S \times 1)$, where S is the number of boundary nodes (or the number of the elements of the constant type) along the free edge;

$\mathbf{G}_{\mathbf{BB}}$ and $\mathbf{G}_{\mathbf{BS}}$ are the matrices of the dimension $(2N \times 2N)$ and of the dimension $(2N \times S)$, respectively, grouping boundary integrals and depending on the type of plate boundary, where N is the number of boundary nodes (or the number of the elements of the constant type) and S is the number of boundary elements along free edge;

Δ is the matrix grouping difference operators connecting angles of rotation in tangent direction with deflections of suitable boundary nodes if a plate has a free edge and \mathbf{I} is the unit matrix.

In the computational program, deflections at two neighbouring nodes are used. Hence, for a clamped edge, a simply-supported edge and a free edge, two independent unknowns are always considered. All of the designations are shown in Fig. 3, where the construction of a set of algebraic equations is presented on the example of the constant type of the boundary element.

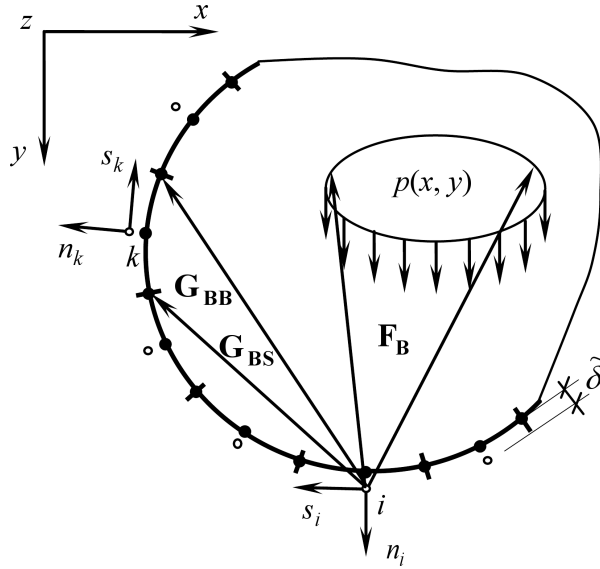


FIG. 3. Assembly of set of algebraic equations in static analysis on the example of the constant type elements.

The boundary integral equation will be formulated in the non-singular approach. To construct the characteristic matrix \mathbf{G} , integration of a suitable fundamental function on the boundary is needed. Integration is done in the local coordinate system n_i, s_i connected with i -th boundary element physical node and next, these integrals must be transformed to n_k, s_k coordinate system, connected with k -th element physical node [31]. Localization of collocation point is defined by the parameter δ or non-dimensional parameter ε . This parameter can be defined as $\varepsilon = \tilde{\delta}/d$ or $\varepsilon = \tilde{\delta}/c$ (Fig. 1).

To calculate elements of the characteristic matrix the following methods are applied: a) classic, numerical Gauss procedure for non-quasi diagonal elements or b) modified, numerical integration of Gauss method for quasi-diagonal elements proposed by LITEWKA and SYGULSKI [31]. The authors proposed inverse localization of Gauss points in the domain of integration. Boundary integrals on a curved element are calculated according to Gauss method. Integrals of fundamental functions over the plate edge are calculated using n_i, s_i coordinate system, connected with i -th physical node. Then, they are transformed to n_k, s_k coordinate system [20–24, 30]:

$$(2.23) \quad \begin{aligned} \varphi_{n_k}^* &= \varphi_{n_i}^* \cdot c_{nn} + \varphi_{s_i}^* \cdot c_{ns}, \\ M_{n_k}^* &= M_{n_i}^* \cdot c_{nn}^2 + M_{s_i}^* \cdot c_{ns}^2 + 2 \cdot M_{n_i s_i}^* \cdot c_{nn} \cdot c_{ns}, \\ M_{n_k s_k}^* &= (M_{s_i}^* - M_{n_i}^*) \cdot c_{nn} \cdot c_{ns} + M_{n_i s_i}^* \cdot (c_{nn}^2 - c_{ns}^2), \\ T_{n_k}^* &= T_{n_i}^* \cdot c_{nn} + T_{s_i}^* \cdot c_{ns}, \end{aligned}$$

where $c_{nn} = \cos(n_k, n_i)$ and $c_{ns} = \cos(n_k, s_i)$.

In the case of consideration of a free edge, the angle of rotation in tangent direction can be expressed by deflection of two neighbouring nodes

$$(2.24) \quad \varphi_s^{(i-1)} = \varphi_s^{(i)} = \varphi_s^{(i+1)} = \frac{w_b^{(i+1)} - w_b^{(i)}}{d_{i+1}},$$

where d_i is a projection of section connecting physical nodes (collocation points) i and $i+1$ on the line tangential to the boundary element in collocation point i -th [29, 30].

Application of the Boundary Element Method allows us to introduce in a simple way a boundary support similar to the support at the vicinity of the selected point. Definition of this boundary support for example of simplified curved boundary element is shown on Fig. 4.

The boundary condition is defined as follows: $w = 0$, $\varphi_s = 0$, $\varphi_n \neq 0$, and the unknown boundary values are: shear force T_n and φ_n the angle of rotation in direction n , which is identical to the definition of part of a simply-supported edge.

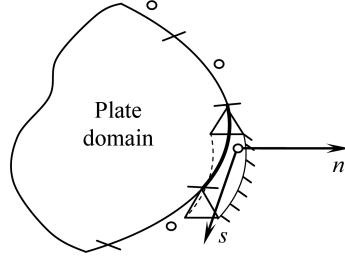


FIG. 4. Boundary support at the vicinity of the selected point.

For isoparametric, curvilinear elements (Fig. 1c) during the procedure of aggregation of characteristic matrix \mathbf{G} , values of directional cosines c_{nn} and c_{ns} in the common node k are calculated as the arithmetic mean of the two values assigned to this node [29], (Fig. 5):

$$(2.25) \quad c_{nn} = \frac{c_{nn}^{(i)} + c_{nn}^{(i+1)}}{2}, \quad c_{ns} = \frac{c_{ns}^{(i)} + c_{ns}^{(i+1)}}{2}.$$

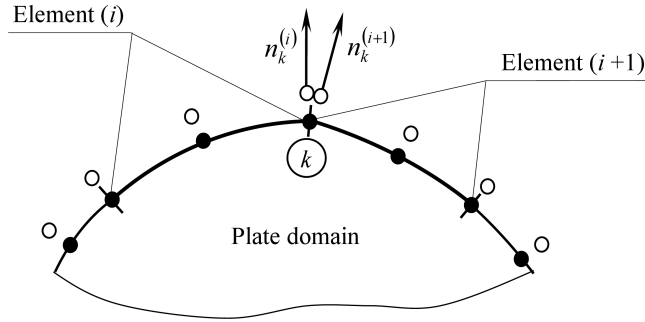


FIG. 5. Construction of the characteristic matrix. Calculation of the directional cosines in the common node [29].

It is assumed that the loading p is acting on a plate surface and has a constant distribution. Integrals

$$p(\mathbf{y}) \cdot \int_{\Omega} w^*(\mathbf{x}, \mathbf{y}) \cdot d\Omega(\mathbf{y}) \quad \text{and} \quad p(\mathbf{y}) \cdot \int_{\Omega} \bar{w}^*(\mathbf{x}, \mathbf{y}) \cdot d\Omega(\mathbf{y})$$

taking place in Eqs. (2.17) and (2.18) can be evaluated analytically in terms of Abdel-Akher and Hartley's proposition (contour of loading is expressed in polygonal form) [32].

2.3. *Calculation of deflection, angle of rotation, bending and twisting moments inside a plate domain*

The solution of the set of algebraic equations allows us to determine boundary variables. Then, it is possible to calculate the deflection, angle of rotation in an arbitrary direction, bending and torsional moments and shear forces at an arbitrary point of the plate domain. Each value can be expressed as the sum of two variables depending on the boundary variables $\bar{\mathbf{B}}$ and external loading p . For example, the deflection can be expressed in the form

$$(2.26) \quad w = w(\bar{\mathbf{B}}, p)$$

which can be calculated directly using boundary integral Eq. (2.17). A similar relation can be applied to establish the angle of rotation in an arbitrary direction

$$(2.27) \quad \varphi_\xi = \varphi_\xi(\bar{\mathbf{B}}, p)$$

which is equivalent to differentiate boundary integral Eq. (2.17) with respect to ξ co-ordinate.

In terms of the thin plate theory, bending moments and torsional moment are given in the classic form

$$(2.28) \quad \begin{aligned} M_x(x, y) &= -D \cdot (w_{,xx} + \nu \cdot w_{,yy}), \\ M_y(x, y) &= -D \cdot (w_{,yy} + \nu \cdot w_{,xx}), \\ M_{xy}(x, y) &= -D \cdot (1 - \nu) \cdot w_{,xy} \end{aligned}$$

and $w(x, y)$ is the function of displacements and x, y are the global coordinates of an arbitrary point. To establish the bending and torsional moments at the point inside a plate domain, it is necessary to double differentiate the boundary integral Eq. (2.17) with respect to x, y , or x and y co-ordinates. As a result, the bending and torsional moments can be expressed by the boundary $\bar{\mathbf{B}}$ and domain p variables

$$(2.29) \quad \begin{aligned} M_x &= M_x(\bar{\mathbf{B}}, p), \\ M_y &= M_y(\bar{\mathbf{B}}, p), \\ M_{xy} &= M_{xy}(\bar{\mathbf{B}}, p). \end{aligned}$$

The shear forces can be calculated according to thin plate theory

$$(2.30) \quad \begin{aligned} Q_x &= \frac{\partial M_x(x, y)}{\partial x} + \frac{\partial M_{yx}(x, y)}{\partial y} = -D \cdot (w_{,xxx} + w_{,xyy}), \\ Q_y &= \frac{\partial M_y(x, y)}{\partial y} - \frac{\partial M_{xy}(x, y)}{\partial x} = -D \cdot (w_{,yxx} + w_{,yyy}) \end{aligned}$$

and they can be expressed in the form

$$(2.31) \quad \begin{aligned} Q_x &= Q_x(\bar{\mathbf{B}}, p), \\ Q_y &= Q_y(\bar{\mathbf{B}}, p) \end{aligned}$$

which calculation of domain variables was described widely in [30].

3. FREE VIBRATION ANALYSIS OF THIN PLATES

The free vibration problem of a thin plate is considered. Inside a plate domain additional collocation points associated with lumped masses are introduced. In each i -th internal collocation point, the vectors of displacement $w_i(t)$, acceleration $\ddot{w}_i(t)$, and inertial force $P_i(t)$ are established

$$(3.1) \quad \begin{aligned} w_i(t) &= W_i \cdot \sin \omega t, \\ \ddot{w}_i(t) &= -\omega^2 \cdot W_i \cdot \sin \omega t, \\ P_i(t) &= P_i \cdot \sin \omega t \end{aligned}$$

and the inertial force amplitude is described

$$(3.2) \quad P_i = \omega^2 \cdot m_i \cdot W_i,$$

where ω is the plate natural frequency and t is the time.

The boundary-domain integral equations have the character of amplitude equations and they are presented in the forms:

$$(3.3) \quad \begin{aligned} c(\mathbf{x}) \cdot w(\mathbf{x}) + \int_{\Gamma} \left[T_n^*(\mathbf{y}, \mathbf{x}) \cdot w(\mathbf{y}) - M_{ns}^*(\mathbf{y}, \mathbf{x}) \cdot \frac{dw(\mathbf{y})}{ds} - M_n^*(\mathbf{y}, \mathbf{x}) \cdot \varphi_n(\mathbf{y}) \right] \\ \cdot d\Gamma(\mathbf{y}) = \int_{\Gamma} \left[\tilde{T}_n(\mathbf{y}) \cdot w^*(\mathbf{y}, \mathbf{x}) - M_n(\mathbf{y}) \cdot \varphi_n^*(\mathbf{y}, \mathbf{x}) \right] \cdot d\Gamma(\mathbf{y}) \\ + \sum_{i=1}^I P_i \cdot w^*(i, \mathbf{x}), \end{aligned}$$

$$(3.4) \quad \begin{aligned} c(\mathbf{x}) \cdot \varphi_n(\mathbf{x}) + \int_{\Gamma} \left[\bar{T}_n^*(\mathbf{y}, \mathbf{x}) \cdot w(\mathbf{y}) - \bar{M}_{ns}^*(\mathbf{y}, \mathbf{x}) \cdot \frac{dw(\mathbf{y})}{ds} - \bar{M}_n^*(\mathbf{y}, \mathbf{x}) \cdot \varphi_n(\mathbf{y}) \right] \\ \cdot d\Gamma(\mathbf{y}) = \int_{\Gamma} \left[\tilde{\bar{T}}_n(\mathbf{y}) \cdot \bar{w}^*(\mathbf{y}, \mathbf{x}) - M_n(\mathbf{y}) \cdot \bar{\varphi}_n^*(\mathbf{y}, \mathbf{x}) \right] \cdot d\Gamma(\mathbf{y}) \\ + \sum_{i=1}^I P_i \cdot w^*(i, \mathbf{x}). \end{aligned}$$

3.1. Assembly of a set of algebraic equations

The set of algebraic equations in a matrix notation has the following form, (Fig. 6):

$$(3.5) \quad \begin{bmatrix} \mathbf{G}_{BB} & \mathbf{G}_{BS} & -\lambda \cdot \mathbf{G}_{Bw} \cdot \mathbf{M}_p \\ \Delta & -\mathbf{I} & \mathbf{0} \\ \mathbf{G}_{wB} & \mathbf{G}_{wS} & -\lambda \cdot \mathbf{G}_{ww} \cdot \mathbf{M}_p + \mathbf{I} \end{bmatrix} \cdot \begin{Bmatrix} \mathbf{B} \\ \boldsymbol{\varphi}_s \\ \mathbf{W} \end{Bmatrix} = \begin{Bmatrix} \mathbf{0} \\ \mathbf{0} \\ \mathbf{0} \end{Bmatrix},$$

where

\mathbf{B} and $\boldsymbol{\varphi}_s$ are the vectors of the amplitudes of the boundary variables;

\mathbf{W} is the vector of the amplitudes of internal deflections associated with lumped masses;

\mathbf{G}_{BB} and \mathbf{G}_{BS} are dimension matrices of the dimensions $(2N \times 2N)$ and $(2N \times S)$ grouping boundary integrals and depend on type of boundary, where N is the number of boundary nodes (or the number of elements of the constant type) and S is the number of boundary elements along a free edge;

\mathbf{G}_{Bw} is the matrix of the dimension $(2N \times M)$ grouping values of the fundamental function w^* established at internal collocation points;

Δ is the matrix grouping difference operators connecting angle of rotations in tangent direction with deflections of suitable boundary nodes if a plate has a free edge;

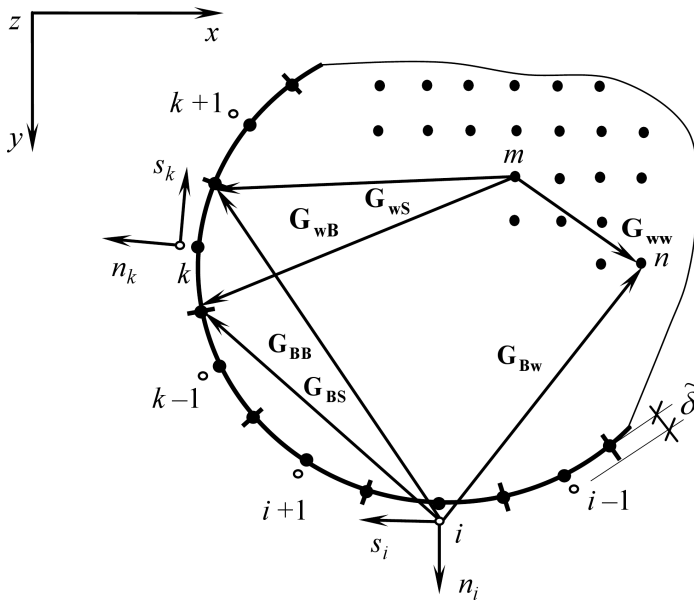


FIG. 6. Assembly of the set of algebraic equations in free vibration analysis on the example of the constant type boundary elements.

$\mathbf{G}_{\mathbf{wB}}$ is the matrix of the dimension $(M \times 2N)$ grouping the boundary integrals of the appropriate fundamental functions, where M is the number of the internal collocation points and N is the number of the boundary nodes;

$\mathbf{G}_{\mathbf{wS}}$ is the matrix of the dimension $(M \times S)$ grouping the boundary integrals of the appropriate fundamental functions;

$\mathbf{G}_{\mathbf{ww}}$ is the matrix of the dimension $(M \times M)$ grouping the values of the fundamental function w^* established at internal collocation points;

$\mathbf{M}_p = \text{diag}(m_1, m_2, m_3, \dots, m_M)$ is a plate mass matrix, $\lambda = \omega^2$ and \mathbf{I} is the unit matrix (M is the number of lumped masses).

Elimination of boundary variables \mathbf{B} and $\boldsymbol{\varphi}_s$ from matrix Eq. (3.5) leads to a standard eigenvalue problem

$$(3.6) \quad \{\mathbf{A} - \tilde{\lambda} \cdot \mathbf{I}\} \cdot \mathbf{W} = \mathbf{0},$$

where

$$(3.7) \quad \mathbf{A} = \left\{ \mathbf{G}_{\mathbf{ww}} \cdot \mathbf{M}_p - (\mathbf{G}_{\mathbf{wB}} - \mathbf{G}_{\mathbf{wS}} \cdot \boldsymbol{\Delta}) \cdot [\mathbf{G}_{\mathbf{BB}} + \mathbf{G}_{\mathbf{BS}}]^{-1} \cdot \mathbf{G}_{\mathbf{Bw}} \cdot \mathbf{M}_p \right\}.$$

4. NUMERICAL EXAMPLES

Circular and elliptic plates with various boundary conditions are considered. Twenty Gauss points are applied to evaluate boundary integrals. The contour of the circular plate is divided by 32 and 64 boundary elements with the same length. For an elliptic plate, localization of geometrical edge nodes for 32 boundary elements is presented in the Fig. 7. For 64 boundary elements, similar localization is assumed, dividing all of segments: l , $l/2$, $l/3$, and $l/6$ by halves.

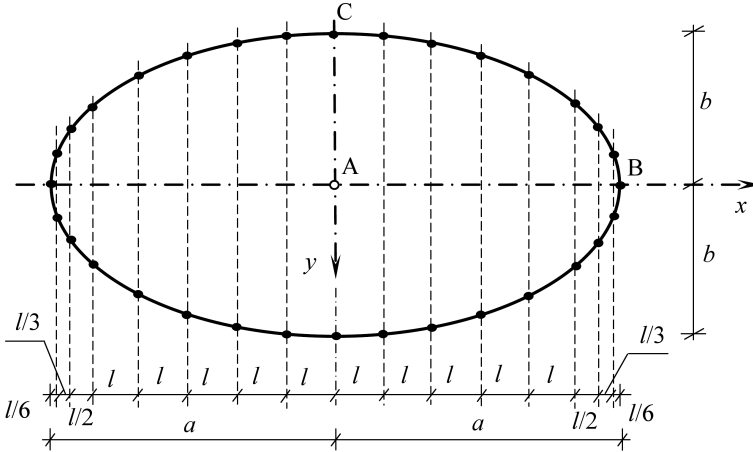


FIG. 7. Localization of boundary elements inscribed in ellipse contour [30].

The following plate properties are assumed: $E = 205.0$ GPa, $\nu = 0.3$, $\rho_p = 7850$ kg/m³, thickness $h_p = 0.01$ m. Circular plate radius $a = 2.0$ m. For the elliptic plate the lengths of the half-axis: $a = 3.0$ m and $b = 2.0$ m. The numerical analysis was conducted using the following boundary and finite element discretisation:

- BEM I – rectilinear boundary element of the constant type, $\varepsilon = \tilde{\delta}/d = 0.1$;
- BEM II – rectilinear boundary element of the constant type, the second boundary-domain Eq. (2.18) for static and (3.4) for free vibration analysis are obtained for the set of two collocation points assigned to each single boundary element with the same fundamental solution w^* , localization of two collocation points for a single boundary element is determined by: $\varepsilon_1 = \tilde{\delta}_1/d = 0.01$ and $\varepsilon_2 = \tilde{\delta}_2/d = 0.1$;
- BEM III – curved, simplified boundary element of the constant type, $\varepsilon = \tilde{\delta}/c = 0.1$;
- BEM IV – three-node isoparametric curved boundary element, $\varepsilon = \tilde{\delta}/c = 0.1$;
- FEM – eight-node doubly curved shell finite element with reduced integration (S8R), Abaqus/STANDARD v6.12 computational program [34]. The circular plate domain was divided into 3936 finite elements.

4.1. Static analysis

Circular and elliptic plates are considered. The geometry, material properties and discretisation are assumed above according to Sec. 4. All plates are subjected only to the uniformly distributed loading $p = 1.0$ kN/m² acting on all domain surface. The results of calculations as deflection and bending moments are presented in the non-dimensional parameters.

4.1.1. *Circular plate clamped on boundary.* The results of calculation are presented in Tables 1–3.

Table 1. Deflection at the plate centre.

| Number of boundary elements | $\tilde{w} = wD/pa^4$ | | | | |
|-----------------------------|-----------------------|-----------|--------------|-----------|--------------------------|
| | BEM I [30] | BEM II | BEM III [30] | BEM IV | Analytical solution [33] |
| 32 | 0.0153482 | 0.0153778 | 0.0156219 | 0.0156220 | 0.0156250 |
| 64 | 0.0155502 | 0.0155639 | 0.0156210 | 0.0156231 | |

Table 2. Bending moment at the plate centre.

| Number of boundary elements | $\widetilde{M}_r = M_r/pa^2$ | | | | Analytical solution [33] |
|-----------------------------|------------------------------|-----------|--------------|-----------|--------------------------|
| | BEM I [30] | BEM II | BEM III [30] | BEM IV | |
| 32 | 0.0812583 | 0.0806215 | 0.0812634 | 0.0812592 | 0.0812500 |
| 64 | 0.0812528 | 0.0810958 | 0.0812545 | 0.0812510 | |

Table 3. Bending moment on boundary.

| Number of boundary elements | $\widetilde{M}_r = M_r/pa^2$ | | | | Analytical solution [33] |
|-----------------------------|------------------------------|-----------|--------------|-----------|--------------------------|
| | BEM I [30] | BEM II | BEM III [30] | BEM IV | |
| 32 | -0.125187 | -0.124077 | -0.123913 | -0.125206 | -0.125000 |
| 64 | -0.125033 | -0.124785 | -0.124823 | -0.124961 | |

4.1.2. *Circular plate simply-supported on boundary.* The results of calculation are presented in Tables 4 and 5.

Table 4. Deflection at the plate centre.

| Number of boundary elements | $\widetilde{w} = wD/pa^4$ | | | | Analytical solution [33] |
|-----------------------------|---------------------------|-----------|--------------|--------|--------------------------|
| | BEM I [30] | BEM II | BEM III [30] | BEM IV | |
| 32 | 0.0598860 | 0.0613256 | 0.0598683 | | 0.0637019 |
| 64 | 0.0620345 | 0.0627804 | 0.0631792 | | |

Table 5. Bending moment at the plate centre.

| Number of boundary elements | $\widetilde{M}_r = M_r/pa^2$ | | | | Analytical solution [33] |
|-----------------------------|------------------------------|----------|--------------|--------|--------------------------|
| | BEM I [30] | BEM II | BEM III [30] | BEM IV | |
| 32 | 0.214596 | 0.201167 | 0.198221 | | 0.206250 |
| 64 | 0.207696 | 0.204218 | 0.204911 | | |

4.1.3. *Circular plate supported at three points on boundary.* The circular plate supported at three points on boundary is considered (Fig. 8).

The results of calculation are presented in Tables 6 and 7. The following designation is assumed $P = pa^2 \cdot \pi$.

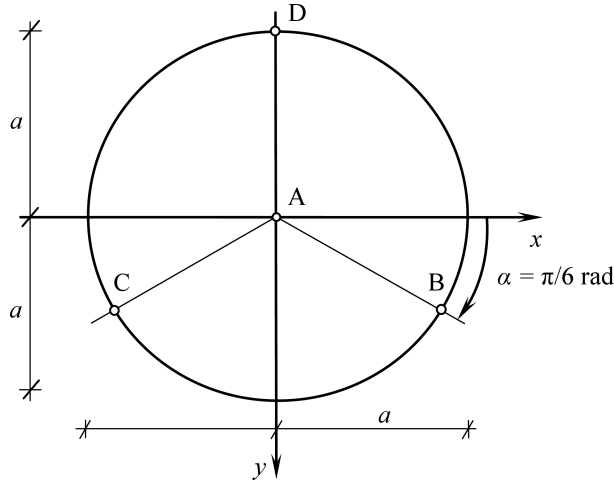


FIG. 8. Circular plate supported at three points on boundary.

Table 6. Deflection at the plate centre.

| Number of boundary elements | $\tilde{w}_A = w_A D / P a^2$ | | | |
|-----------------------------|-------------------------------|---------|---------|--------------------------|
| | BEM I | BEM II | BEM III | Analytical solution [33] |
| 64 | 0.03636 | 0.03655 | 0.03637 | 0.03620 |

Table 7. Principal moments at the plate centre.

| Number of boundary elements | BEM I | BEM II | BEM III |
|---------------------------------|----------|----------|----------|
| $\tilde{M}_{IA} = M_{IA} / P$ | | | |
| 64 | 0.070077 | 0.070580 | 0.071305 |
| $\tilde{M}_{IIA} = M_{IIA} / P$ | | | |
| 64 | 0.058872 | 0.059355 | 0.060209 |

4.1.4. *Elliptic plate clamped on boundary.* The results of calculation are presented in Tables 8–10.

Table 8. Deflection at the plate centre.

| Number of boundary elements | $\tilde{w}_A = w_A D / p b^4$ | | | |
|-----------------------------|-------------------------------|-----------|--------------|--------------------------|
| | BEM I [30] | BEM II | BEM III [30] | Analytical solution [33] |
| 32 | 0.0274325 | 0.0274708 | 0.0278863 | 0.0278926 |
| 64 | 0.0275220 | 0.0275314 | 0.0278648 | |

Table 9. Bending moment at the plate centre.

| Number of boundary elements | BEM I [30] | BEM II | BEM III [30] | Analytical solution [33] |
|------------------------------------|------------|-----------|--------------|--------------------------|
| $\widetilde{M}_{xA} = M_{xA}/pb^2$ | | | | |
| 32 | 0.0826588 | 0.0826889 | 0.0830993 | 0.0830578 |
| 64 | 0.0828583 | 0.0827314 | 0.0830984 | |
| $\widetilde{M}_{yA} = M_{yA}/pb^2$ | | | | |
| 32 | 0.125312 | 0.125379 | 0.126464 | 0.126446 |
| 64 | 0.125879 | 0.125523 | 0.126463 | |

Table 10. Bending moment on boundary.

| Number of boundary elements | BEM I [30] | BEM II | BEM III [30] | Analytical solution [33] |
|------------------------------------|------------|-----------|--------------|--------------------------|
| $\widetilde{M}_{xB} = M_{xB}/pb^2$ | | | | |
| 32 | -0.103246 | -0.102141 | -0.102433 | -0.0991735 |
| 64 | -0.101109 | -0.100700 | -0.101110 | |
| $\widetilde{M}_{yC} = M_{yC}/pb^2$ | | | | |
| 32 | -0.220628 | -0.220663 | -0.222646 | -0.223140 |
| 64 | -0.221884 | -0.221363 | -0.222647 | |

4.1.5. *Elliptic plate simply-supported on boundary.* The results of calculation are presented in Tables 11 and 12.

Table 11. Deflection at the plate centre.

| Number of boundary elements | $\widetilde{w}_A = w_A D/pb^4$ | | | |
|-----------------------------|--------------------------------|----------|--------------|--------------------------|
| | BEM I [30] | BEM II | BEM III [30] | Analytical solution [33] |
| 32 | 0.110148 | 0.111084 | 0.116411 | 0.115385 |
| 64 | 0.112546 | 0.111688 | 0.116395 | |

Table 12. Bending moment at the plate centre.

| Number of boundary elements | BEM I [30] | BEM II | BEM III [30] | Analytical solution [33] |
|------------------------------------|------------|----------|--------------|--------------------------|
| $\widetilde{M}_{xA} = M_{xA}/pb^2$ | | | | |
| 32 | 0.213114 | 0.214340 | 0.219376 | 0.222000 |
| 64 | 0.213915 | 0.215354 | 0.222126 | |
| $\widetilde{M}_{yA} = M_{yA}/pb^2$ | | | | |
| 32 | 0.356133 | 0.343355 | 0.353365 | 0.379000 |
| 64 | 0.367544 | 0.344413 | 0.368365 | |

4.2. Free vibration analysis

Circular plates are considered. Geometry, material properties, and discretisation are assumed above according to Sec. 4. Two types of localization of lumped masses are proposed. The first one (a) with 128 lumped masses is presented in Fig. 9. The second one (b) with 112 lumped masses is shown in Fig. 10. The re-

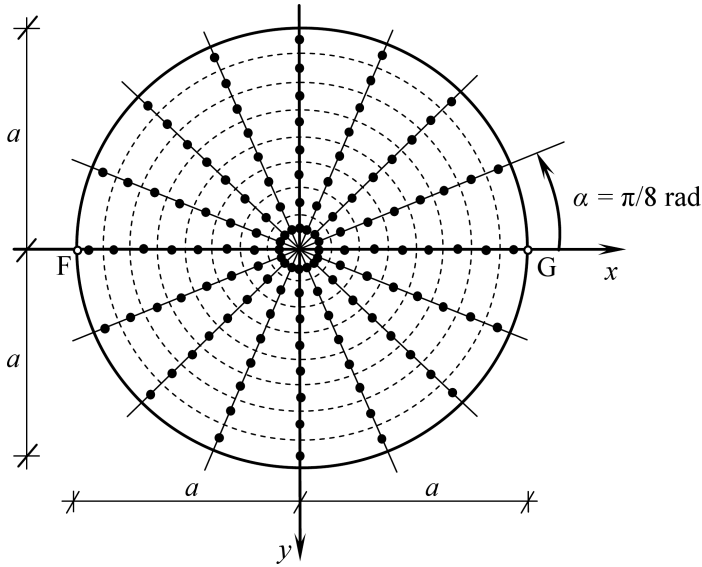


FIG. 9. Lumped masses localization.

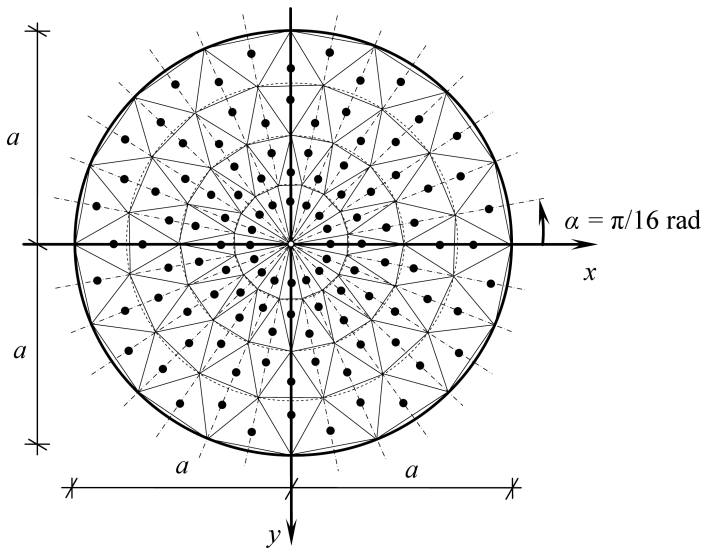


FIG. 10. Discretization into sub-domains and lumped masses localization.

sults of calculations as natural frequencies are presented in the non-dimensional parameters. The i -th natural frequency is expressed in terms of parameter μ_i :

$$\omega_i = \frac{\mu_i}{a^2} \cdot \sqrt{\frac{D}{\rho_p \cdot h_p}},$$

where ρ_p is a plate density. The modes are presented as two-dimensional graphs of displacements located along x axis between points F and G (Fig. 9).

According to the analytical approach for continuous mass distribution and axisymmetric boundary conditions, the natural frequencies can be expressed as the two-index object ω_{mn} , where m and n are the numbers of the nodal diameters and circles respectively. The values of calculated ω_i according to the BEM and FEM approach corresponding to the respective values of ω_{mn} . In the tables, the respective values of ω_{mn} are indicated using the non-dimensional parameters μ_{mn} .

4.2.1. Circular plate clamped on boundary. The results of calculation are presented in Tables 13–16. The modes are presented in Fig. 11.

Table 13. Comparison of natural frequencies.

| Modes | μ_i | | | | |
|--------------------------|------------------|------------------------|------------------------|------------------|------------------------|
| | 1 (μ_{10}) | 2 and 3 (μ_{11}) | 4 and 5 (μ_{12}) | 6 (μ_{20}) | 7 and 8 (μ_{21}) |
| BEM I(a) | 10.1696 | 21.2822 | 34.7940 | 39.1814 | 50.5116 |
| BEM I(b) | 10.1711 | 21.6720 | 36.0846 | 40.6116 | 52.4364 |
| BEM II(a) | 10.1679 | 21.2828 | 34.7961 | 39.1749 | 50.5140 |
| BEM II(b) | 10.1679 | 21.6708 | 36.0844 | 40.5977 | 52.4363 |
| BEM III(a) | 10.1499 | 21.2437 | 34.7321 | 39.1065 | 50.4221 |
| BEM III(b) | 10.1503 | 21.6320 | 36.0164 | 40.5184 | 52.3363 |
| FEM | 10.2199 | 21.2681 | 34.8840 | 39.7817 | 51.0338 |
| Analytical solution [35] | 10.1679 | 21.7940 | 34.8460 | 39.7552 | 60.8490 |

Table 14. Influence of the parameter ε on the results of calculation μ_i , BEM I(a).

| $\varepsilon = \tilde{\delta}/c$ | | 0.01 | 0.05 | 0.1 | 0.2 | 0.5 |
|----------------------------------|---------|---------|---------|---------|---------|---------|
| Modes | 1 | 10.1727 | 10.1711 | 10.1696 | 10.1674 | 10.1652 |
| | 2 and 3 | 21.2857 | 21.2840 | 21.2822 | 21.2798 | 21.2768 |
| | 4 and 5 | 34.7983 | 34.7962 | 34.7940 | 34.7909 | 34.7868 |
| | 6 | 39.1923 | 39.1870 | 39.1814 | 39.1736 | 39.1646 |
| | 7 and 8 | 50.5165 | 50.5141 | 50.5116 | 50.5080 | 50.5028 |

Table 15. Influence of the parameter ε on the results of calculation μ_i , BEM III(a).

| $\varepsilon = \tilde{\delta}/c$ | | 0.01 | 0.05 | 0.1 | 0.2 | 0.5 |
|----------------------------------|---------|---------|---------|---------|---------|---------|
| Modes | 1 | 10.1514 | 10.1482 | 10.1499 | 10.1501 | 10.1492 |
| | 2 and 3 | 21.2454 | 21.2415 | 21.2437 | 21.2442 | 21.2431 |
| | 4 and 5 | 34.7341 | 34.7288 | 34.7321 | 34.7332 | 34.7319 |
| | 6 | 39.1121 | 39.0998 | 39.1065 | 39.1077 | 39.1042 |
| | 7 and 8 | 50.4241 | 50.4167 | 50.4221 | 50.4246 | 50.4237 |

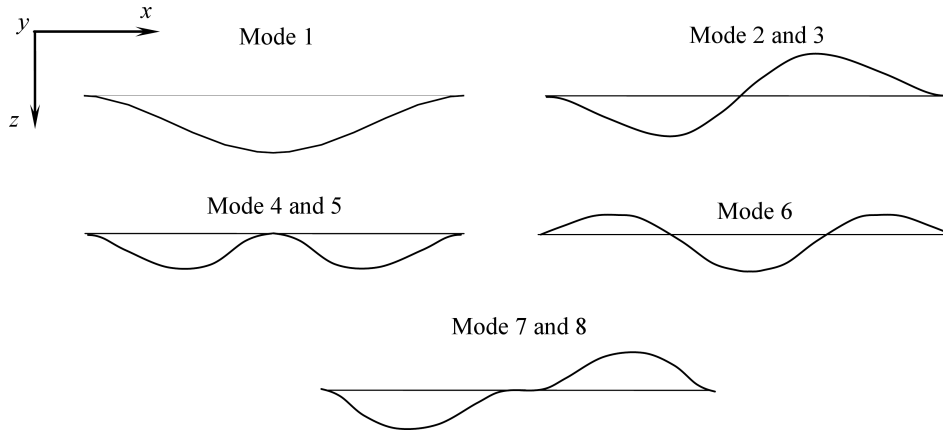


FIG. 11. Circular plate clamped on the whole edge. Modes 1–8, BEM III(a).

4.2.2. *Circular plate simply-supported on boundary.* The results of calculation are presented in Tables 16–18. The modes are presented in Fig. 12.

Table 16. Comparison of natural frequencies.

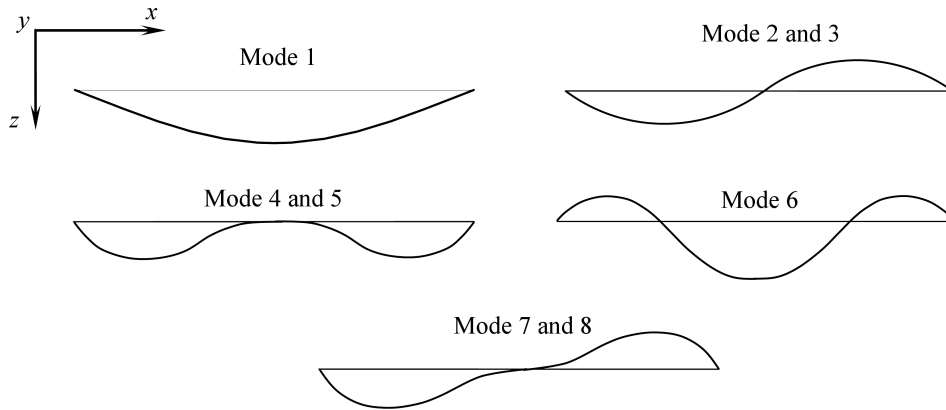
| Modes | μ_i | | | | |
|------------|------------------|------------------------|------------------------|------------------|------------------------|
| | 1 (μ_{10}) | 2 and 3 (μ_{11}) | 4 and 5 (μ_{12}) | 6 (μ_{20}) | 7 and 8 (μ_{21}) |
| BEM I(a) | 4.9695 | 13.9162 | 25.5664 | 29.3974 | 39.6172 |
| BEM I(b) | 5.0132 | 14.2108 | 26.2463 | 29.5917 | 40.5584 |
| BEM II(a) | 4.9498 | 13.9162 | 25.5649 | 29.3808 | 39.6152 |
| BEM II(b) | 4.9868 | 14.2109 | 26.2466 | 29.5684 | 40.5586 |
| BEM III(a) | 4.8935 | 13.8920 | 25.5455 | 29.2894 | 39.5860 |
| BEM III(b) | 4.9303 | 14.1856 | 26.2240 | 29.4674 | 40.5243 |
| FEM | 4.9358 | 13.9011 | 25.6108 | 29.7301 | 39.9434 |

Table 17. Influence of the parameter ε on the results of calculation μ_i . BEM III(a).

| $\varepsilon = \tilde{\delta}/c$ | | 0.01 | 0.05 | 0.1 | 0.2 | 0.5 |
|----------------------------------|---------|---------|---------|---------|---------|---------|
| Modes | 1 | 4.9815 | 4.9763 | 4.9695 | 4.9569 | 4.9329 |
| | 2 and 3 | 13.9160 | 13.9161 | 13.9162 | 13.9162 | 13.9154 |
| | 4 and 5 | 25.5632 | 25.5647 | 25.5664 | 25.5696 | 25.5751 |
| | 6 | 29.4055 | 29.4021 | 29.3974 | 29.3878 | 29.3659 |
| | 7 and 8 | 39.6126 | 39.6149 | 39.6172 | 39.6207 | 39.6273 |

Table 18. Influence of the parameter ε on the results of calculation μ_i . BEM III(a).

| $\varepsilon = \tilde{\delta}/c$ | | 0.01 | 0.05 | 0.1 | 0.2 | 0.5 |
|----------------------------------|---------|---------|---------|---------|---------|---------|
| Modes | 1 | 6.9839 | 4.8250 | 4.8935 | 4.9185 | 4.9234 |
| | 2 and 3 | 13.8487 | 13.8925 | 13.8920 | 13.8922 | 13.8924 |
| | 4 and 5 | 24.4712 | 25.5704 | 25.5455 | 25.5360 | 25.5329 |
| | 6 | 31.5309 | 29.2350 | 29.2894 | 29.3107 | 29.3156 |
| | 7 and 8 | 37.7022 | 39.6282 | 39.5860 | 39.5688 | 39.5608 |

**FIG. 12.** Circular plate simply-supported on the whole edge. Modes 1–8, BEM III(a).

4.2.3. Circular plate supported at three points on boundary. The circular plate supported at three points on a boundary is considered (Fig. 8). The results of calculation are presented in Tables 19–21. The modes are presented in the Fig. 14 where displacements along x axis are shown. Additionally, to compare the results of calculation, free vibration of a circular plate resting on three column supports will be considered. The column support will be introduced according to the Bèzine approach and free vibrations analysis presented in [24] as a sub-domain with one collocation point. The rectilinear boundary element in the non-singular approach for $\varepsilon = \tilde{\delta}/c = 0.1$ is introduced and designed as BEM I*.

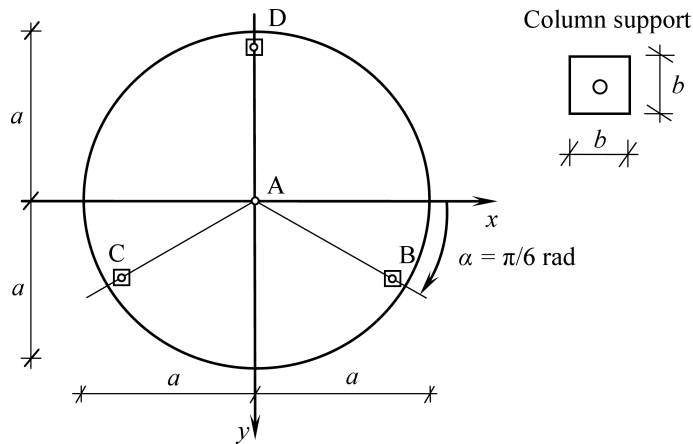


FIG. 13. Circular plate supported at three internal column supports located near the free boundary.

Table 19. Comparison of natural frequencies.

| μ_i | | | | | | | | |
|------------|--------|--------|--------|---------|---------|---------|---------|---------|
| Modes | 1 | 2 | 3 | 4 | 5 | 6 | 7 | 8 |
| BEM I(a) | 3.1354 | 3.4062 | 3.4306 | 10.1162 | 11.8526 | 12.7345 | 12.9057 | 21.2721 |
| BEM I(b) | 3.1361 | 3.4022 | 3.4459 | 10.0428 | 11.8373 | 12.7697 | 12.9821 | 21.4804 |
| BEM II(a) | 3.1326 | 3.4054 | 3.4225 | 10.0991 | 11.8514 | 12.7331 | 12.9045 | 21.2713 |
| BEM II(b) | 3.1336 | 3.4014 | 3.4375 | 10.0260 | 11.8362 | 12.7684 | 12.9809 | 21.4795 |
| BEM III(a) | 3.0858 | 3.3570 | 3.3671 | 10.1430 | 11.7724 | 12.6584 | 12.8644 | 21.2652 |
| BEM III(b) | 3.1572 | 3.4308 | 3.4528 | 10.0704 | 11.9436 | 12.8740 | 13.0733 | 21.5872 |
| BEM I*(a) | 3.4552 | 3.4952 | 4.0123 | 10.0611 | 12.4699 | 14.0594 | 14.4777 | 21.2279 |
| BEM I*(b) | 3.4390 | 3.4390 | 4.0132 | 9.9417 | 12.3835 | 14.1293 | 14.5609 | 21.3180 |
| FEM | 2.8765 | 3.7190 | 3.8089 | 10.0325 | 10.3183 | 13.9123 | 13.9153 | 20.7820 |

Table 20. Influence of the parameter ε on the results of calculation μ_i , BEM I(a).

| $\varepsilon = \tilde{\delta}/c$ | | 0.2 | 0.5 | 1.0 |
|----------------------------------|---|---------|---------|---------|
| Modes | 1 | 3.1315 | 3.1354 | 3.1608 |
| | 2 | 3.4024 | 3.4062 | 3.4373 |
| | 3 | 3.4230 | 3.4306 | 3.4444 |
| | 4 | 10.1034 | 10.1162 | 10.1399 |
| | 5 | 11.8222 | 11.8526 | 11.9587 |
| | 6 | 12.6992 | 12.7345 | 12.8449 |
| | 7 | 12.8767 | 12.9057 | 13.0069 |
| | 8 | 21.2570 | 21.2721 | 21.3779 |

Table 21. Influence of the parameter ε on the results of calculation μ_i , BEM III(a).

| $\varepsilon = \tilde{\delta}/c$ | | 0.2 | 0.5 | 1.0 |
|----------------------------------|---|---------|---------|---------|
| Modes | 1 | 2.9532 | 3.0858 | 3.1557 |
| | 2 | 3.1166 | 3.3570 | 3.4347 |
| | 3 | 3.1728 | 3.3671 | 3.4380 |
| | 4 | 10.1883 | 10.1430 | 10.1444 |
| | 5 | 11.2658 | 11.7724 | 11.9549 |
| | 6 | 12.2287 | 12.6584 | 12.8371 |
| | 7 | 12.5438 | 12.8644 | 12.9937 |
| | 8 | 20.9594 | 21.2652 | 21.3818 |

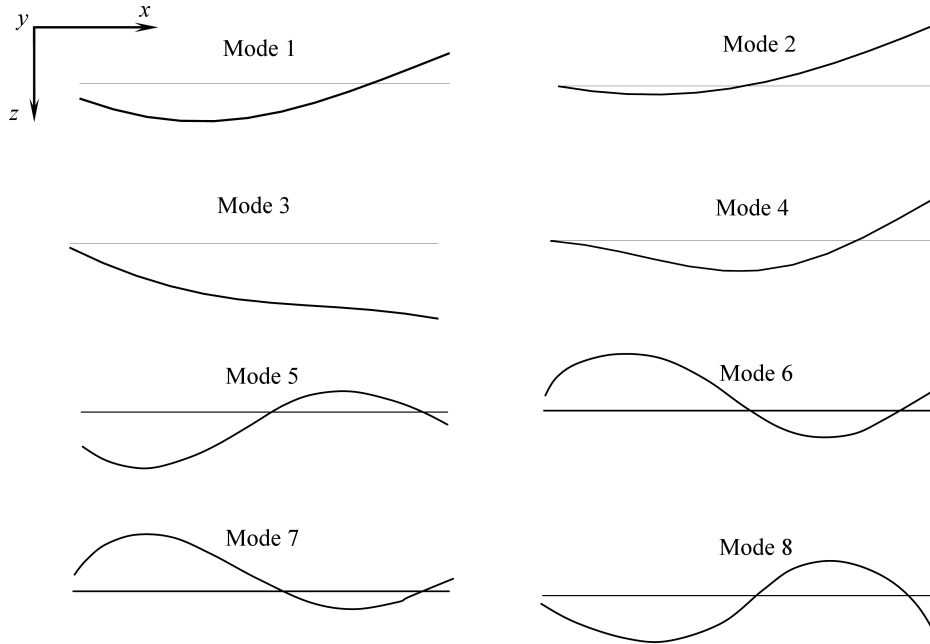


FIG. 14. Circular plate supported at three points on boundary. Modes 1–8, BEM III(a).

Localisation of three identical square column support is presented in the Fig. 13. The co-ordinates of the centres of three column supports are:

$$x_B = 1.602 \text{ m}, \quad y_B = 0.925 \text{ m};$$

$$x_C = -1.602 \text{ m}, \quad y_C = 0.925 \text{ m};$$

$$x_D = 0.0 \text{ m}, \quad y_D = -1.9 \text{ m}.$$

The dimension of the side of the column cross-section is equal $b = 0.1 \text{ m}$.

5. CONCLUSIONS

The static and free vibration analyses of thin plates using the Boundary Element Method were presented. These problems were solved with the modified, alternative approach, in which the boundary conditions are defined so that there is no need to introduce equivalent boundary quantities dictated by the boundary value problem for the biharmonic differential equation. The collocation version of the Boundary Element Method with non-singular calculations of the boundary integrals was employed. The Bèzine technique was used to establish the vector of inertial forces inside a plate. The high number of boundary elements and internal sub-surfaces are not required to obtain sufficient accuracy. In the free vibration analysis it can be observed that regular, radial localisation of lumped masses (Fig. 9) gives more accurate results, close to the analytical and FEM solution for the clamped plate. For the plate simply-supported along all edges the corresponding natural frequencies take similar values for both types of lumped masses localisations. Some divergence of the first natural frequency results obtained using BEM and FEM approach can be observed for the plate supported on three points on a boundary. The influence of non-dimensional parameter ε on obtained results was presented, too. For the static analysis, the influence of parameter ε on obtained results and conditioning of characteristic matrix \mathbf{G} was presented in [30]. The vibration problem of thin plate can be also formulated using the fundamental solution describing dynamic behaviour of an infinite plate. This fundamental solution has the form [1]

$$w^*(\mathbf{x}, \mathbf{y}, \omega) = \frac{i \cdot [H_0^{(1)}(\lambda r) - H_0^{(1)}(i \cdot \lambda r)]}{8\lambda^2},$$

where $\lambda^4 = (\omega^2 \cdot \rho_p h_p / D)$ and $H_0^{(1)}$ is the Hankel function of the first kind of order zero. An application of this fundamental solution does not require discretisation of a plate domain but finally, in addition to the calculated natural frequencies, evaluation of displacements inside a plate domain is needed to obtain the plate modes. An application of the static fundamental solution (2.4) and a plate domain discretisation simplifies computational algorithms and provides in a simple way to a standard eigenvalue problem yielding directly eigenvalues and eigenvectors. The presented approach can be applied to solve fluid-structure interaction problems using the Boundary Element Method, too [22].

An application of simple fundamental solution (2.4) allows us to expand the analysed issue to the free or forced vibration problem of plates with variable thickness considering fluid-plate interaction. In this case the Analogue Equation Method connected to the BEM should be applied.

The boundary element results obtained for the present conception of the thin plate bending issue demonstrates the sufficient effectiveness and efficiency of the proposed approach which may be useful in engineering for the static and free vibration analyses of plates with the curved edges.

ACKNOWLEDGMENT

The author thanks Prof. Ryszard Sygulski and Prof. John T. Katsikadelis for conducting and supervising the scientific and engineering research related to the numerical analysis of structures by the BEM.

REFERENCES

1. BURCZYŃSKI T., *The Boundary Element Method in Mechanics* [in Polish], Technical-Scientific Publishing, Warszawa, 1995.
2. WROBEL L.C., ALIABADI M.H., *The Boundary Element Methods in Engineering*, McGraw-Hill College, 2002.
3. KATSIKADELIS J.T., *Boundary Elements: Vol. II, Analysis of Plates* [in Greek: ΣΥΝΟΠΙΑΚΑ ΣΤΟΙΧΕΙΑ, Τομος II: Ανάλυση Πλακών, 2^η Έκδοση, ΕΜΠ 2010], 2nd Edition, NTUA, Athens, 260, 2010.
4. ALTIERO N.J., SIKARSKIE D.L., *A boundary integral method applied to plates of arbitrary plane form*, Computers and Structures, **9**: 163–168, 1978.
5. BÈZINE G., GAMBY D.A., *A new integral equations formulation for plate bending problems*, Advances in Boundary Element Method, Pentech Press, London, 1978.
6. STERN M., *A general boundary integral formulation for the numerical solution of plate bending problems*, International Journal of Solids and Structures, **15**: 769–782, 1978.
7. HARTMANN F., ZOTEMANTEL R., *The direct boundary element method in plate bending*, International Journal of Numerical Method in Engineering, **23**: 2049–2069, 1986.
8. DEBBIH M., *Boundary element method versus finite element method for the stress analysis of plates in bending*, MSc Thesis, Cranfield Institute of Technology, Bedford, 1987.
9. DEBBIH M., *Boundary element stress analysis of thin and thick plates*, PhD Thesis, Cranfield Institute of Technology, Bedford, 1989.
10. BESKOS D.E., *Dynamic analysis of plates by boundary elements*, Applied Mechanics Review, **7**(26): 213–236, 1999.
11. WEN P.H., ALIABADI M.H., YOUNG A., *A boundary element method for dynamic plate bending problems*, International Journal of Solids and Structures, **37**: 5177–5188, 2000.
12. SHI G., *Flexural vibration and buckling analysis of orthotropic plates by the boundary element method*, International Journal of Solids and Structures, **12**(26): 1351–1370, 1990.
13. MYŚLECKI K., OLEŃKIEWICZ J., *Analysis of natural frequencies of thin plate by the Boundary Element Method* [in Polish], Research Problems of Civil Engineering, Publishing House of Białystok University of Technology, Białystok, **2**: 511–516, 2007.

14. OLEŃKIEWICZ J., *Analysis of vibrations of plane girders by the Boundary Element Method, Doctoral dissertation* [in Polish], Wrocław University of Technology, Institute of Civil Engineering, 2011.
15. KATSIKADELIS J.T., *A boundary element solution to the vibration problem of plates*, Journal of Sound and Vibration, **141**(2): 313–322, 1990.
16. KATSIKADELIS J.T., *A boundary element solution to the vibration problem of plates*, International Journal of Solids and Structures, **27**(15): 1867–1878, 1991.
17. KATSIKADELIS J.T., SAPOUNTZAKIS E.J., ZORBA E.G., *A BEM Approach to Static and Dynamic Analysis with Internal Supports*, Computational Mechanics, **7**(1): 31–40, 1990.
18. KATSIKADELIS J.T., KANDILAS C.B., *A flexibility matrix solution of the vibration problem of plates based on the Boundary Element Method*, Acta Mechanica, **83**(1–2): 51–60, 1990.
19. KATSIKADELIS J.T., SAPOUNTZAKIS E.J., *A BEM Solution to dynamic analysis of plates with variable thickness*, Computational Mechanics, **7**(5–6): 369–379, 1991.
20. GUMINIAK M., *Analysis of thin plates by the boundary element method using modified formulation of boundary condition* [in Polish], Doctoral dissertation, Poznań University of Technology, Faculty of Civil Engineering, Architecture and Environmental Engineering, 2004.
21. GUMINIAK M., *Free vibration analysis of thin plates by the Boundary Element Method in non-singular approach*, Scientific Research of the Institute of Mathematics and Computer Science, **1**(6): 75–90, 2007.
22. GUMINIAK M., SYGULSKI R., *Vibrations of system of plates immersed in fluid by BEM*, Proceedings of 3rd European Conference on Computational Mechanics, Solids, Structures and Coupled Problems in Engineering ECCM, 2006, p. 211, C.A. Mota Soares, J.A.C. Rodrigues, J.A.C. Ambrósio, C.A.B. Pina, C.M. Mota Soares, E.B.R. Pereira and J. Folgado [Eds.], CD enclosed, June 5–9, 2006, Lisbon, Portugal.
23. GUMINIAK M., SYGULSKI R., *The analysis of internally supported thin plates by the Boundary Element Method. Part 1 – Static analysis*, Foundations of Civil and Environmental Engineering, **9**: 17–41, 2007.
24. GUMINIAK M., SYGULSKI R., *The analysis of internally supported thin plates by the Boundary Element Method. Part 2 – Free vibration analysis*, Foundation of Civil and Environmental Engineering, **9**: 43–74, 2007.
25. SYGULSKI R., *Dynamic analysis of open membrane structures interacting with air*, International Journal of Numerical Method in Engineering, **37**: 1807–1823, 1994.
26. KATSIKADELIS J.T., *The analog equation method. A powerful BEM-based solution technique for solving linear and nonlinear engineering problems*, [in:] Boundary Element Method, Brebbia C.A. [Ed.], XVI: 167–182, Computational Mechanics Publications, Southampton, 1994.
27. BABOUSKOS N., KATSIKADELIS J.T., *Flutter instability of damped plates under combined conservative and nonconservative loads*, Archive of Applied Mechanics, **79**: 541–556, 2009.
28. KATSIKADELIS J.T., BABOUSKOS N.G., *Nonlinear flutter instability of thin damped plates: A solution by the analog equation method*, Journal of Mechanics of Materials and Structures, **4**(7–8): 1395–1414, 2009.

29. GUMINIAK M., *Application of curved boundary elements in plate analysis* [in Polish], The 2nd Congress of Polish Mechanics, Book of Abstracts, 117, scientific redaction: T. Łodygowski, W. Sumelka, Poznań, 29–31 August 2011, Poland.
30. GUMINIAK M., *Application of the curved boundary elements in static of thin plates*, [in:] Exact curved elements in Finite and Boundary Element Method, scientific redaction: J. Rakowski, Poznań University of Technology Publishing House, Poznań 2011.
31. LITEWKA B., SYGULSKI R., *The Boundary Element Method in static of Reissner plates of non-continuous boundary conditions* [in Polish], The 2nd Congress of Polish Mechanics, Book of Abstracts, 119, scientific redaction: T. Łodygowski, W. Sumelka, Poznań, 29–31 August 2011, Poland.
32. ABDEL-AKHER A., HARTLEY G.A., *Evaluation of boundary integrals for plate bending*, International Journal of Numerical Method in Engineering, **28**: 75–93, 1989.
33. TIMOSHENKO S., WOJNOWSKY-KRIEGER S., *Theory of plates and shells* [in Polish], Arkady, Warszawa, 1962.
34. Abaqus, Abaqus Manuals. Inc. Providence, 2005.
35. NOWACKI W., *Dynamics of structures* [in Polish], Warszawa, Arkady, Warszawa, 1961.

Received August 12, 2014; accepted version March 11, 2015.
